Dynamic excess pore water pressures by dynamic soil masses and dynamic water heights

Phuong H.V. Truong

***Abstract*—** Dynamic excess pore water pressures due to the vertical and horizontal components of earthquakes based on the dynamic water heights and dynamic soil masses increases with the increase in the thickness of liquefiable soil and shear wave velocity of the hard rock; and with the decrease in the density, the Poisson's ratio and bulk modulus of the liquefiable soil, the depth of the earthquake fault and the earthquake frequency. The geotechnical profile has five layers of soils or rock, e.g. hard rock, weathered rock, hard soil, liquefiable soil and top soil.

***Keywords*—**Pore water pressure, liquefaction, bulk modulus, earthquake depth, shear wave velocity, soil density.

I. Introduction

Dynamic excess pore water pressures are normally used to determine the effective stress and to evaluate the liquefaction potential. Zhang et al.[1] have used shaking table tests are performed to investigate the behavior of excess pore water pressure in different soft soil-foundations of soil-structure interaction (SSI) system; and found that (i) the micro-drainage condition in soils generates and develops with the rising of excess pore pressure, (ii) the micro-drainage conditions will restrain the relative increase amplitude of excess pore water pressure in the repeated loading process, and (iii) the peak of excess pore water pressure during the repeated loading process will not be significantly higher than that of the previous cycle. The excess pore water pressure increment between two consecutive load steps, in undrained cyclic loading ring shear test, consists of a cyclic component induced by dynamic stresses and a residual component due to potential of volume reduction with progress of shear displacement (Trandafir et al [2]).

Matsui et al. [3] observed that for a given number of cycles, higher excess pore water pressures are generated at lower frequencies by using the stress-controlled triaxial test equipment, and the excess pore water pressure increases with the increase in the periods of cyclic shear in the two-way controlled cyclic shear tests (Matsuda et al. [4]).

The seismic force applied to the embankment models is very sensitive and the effect on model depends on soil foundation characteristics. The embankment suffers from increasing pore water pressure due to strong dynamic force. Provision of dense layer under the embankment decreases excess pore water pressure. Due to increasing unit weight of sandy soil foundation, stability of the embankment has been increased. One of the economical methods in controlling liquefaction is increasing subsoil density (Namdar et al. [5]).

Engineering practitioners commonly use penetration-based methods (SPT & CPT) for assessment of seismic liquefaction triggering hazard. On the horizon, shear wave velocity (Vs) may offer engineers a third tool that is lower cost and provides more physically meaningful measurements. Development of the shear wave velocity liquefaction method has been hampered by a paucity of published velocity profiles; particularly in deeper soil deposits (>10m) and deposits subjected to high cyclic stress ratios (CSR > 0.3) (Kayen et al. [6]).

This paper is to present the expressions of the dynamic excess pore water pressures (DEPWPs) due to the vertical and horizontal components of earthquakes based on the dynamic soil masses and dynamic water heights (Truong [7, 8, 9, 10, 11, 12, 13 and 14]) for five layers of soils and rocks which vary with the properties of the soil and rock layers and earthquake frequencies. The dynamic soil masses and dynamic water heights are determined based on the shear wave velocities of soil and water.

II. Dynamic Excess Pore Water Pressures

Dynamic excess pore water pressure (DEPWP) based on dynamic water heights (DWHs), dynamic soil heights (DSHs) and dynamic equivalent factors (DEFs) can be defined as:

$$h_e = \frac{H_{s2} h_{s2z}}{(H_r / F_{rs2}) + (H_{wr} / F_{rwr}) + (H_{s3} / F_{s3s2}) + H_{s2}} \quad (1)$$

Where h = mobilized soil height, H = thickness of soil or rock; subscripts z, r, wr, s1, s2, s3 and F are for vertical direction, hard rock, weathered rock, soil No.1, soil No.2, soil No.3 and earthquake fault, respectively; F = dynamic equivalent factor which is the ratio of dynamic hard rock height to weathered rock height or dynamic soil height; subscripts rwr, rs2 and s3s2 are for rock to weathered rock, rock to soil No.2, and soil No.3 to soil No.2, respectively. The soil No.2 is the liquefiable soil which is the soil-air-water (SAW) mixture.

The dynamic equivalent factor (DEF) of the hard rock to the weathered rock due to the vertical component of an earthquake

Manuscript received July 10, 2012: Revised version received Sep. 4, 2012.

Phuong H. V. Truong, Research Engineer, Westminster, CA 92683 USA (phone: 714-829-7097; e-mail: hvptruongya@yahoo.com).

based on the dynamic soil masses (Truong, 2009, 2010, 2011b and c) is

$$F_{zrwr} = \frac{V_{sr}}{\omega_{zr} s_r} \frac{\omega_{zwr} s_{wr}}{V_{swr}} \quad (2)$$

The dynamic equivalent factor (DEF) of the hard rock to the soil due to the vertical component of an earthquake is

$$F_{zrs} = \frac{V_{sr}}{\omega_{zr} s_r} \frac{\omega_{zs} s_s}{V_{ss}} \quad (3)$$

The dynamic equivalent factor (DEF) of the hard rock to the weathered rock due to the horizontal component of an earthquake based on the dynamic soil masses is

$$F_{xrwr} = \frac{V_{sr}}{\omega_{xr}} \frac{\omega_{xwr}}{V_{swr}} \quad (4)$$

Where Vs = shear-wave velocity, ω_x = Circular frequency of the earthquake in horizontal direction, ω_z = Circular frequency of the earthquake in vertical direction, and

$$s = \frac{\sqrt{(1-2\mu)}}{\sqrt{2(1-\mu)}} \quad (5)$$

Where μ = Poisson' ratio of soil.

III. SENSITIVITY STUDY ON DYNAMIC PORE WATER PRESSURES

The fault depth and the approximate Richter magnitude of the 1989 Loma Prieta earthquake is 18 km and 7.0, respectively. The frequencies in vertical and horizontal directions are 0.1 Hz. Other properties of the soil profile, which have three layers: hard rock, weathered rock, soil No.3, liquefiable soil (soil No.2), and top soil (soil No.1), are given in Table 1

Table 1. Properties of the soil profile

Soil Profile	H. Rock	w. Rock	Soil No.3	Liq.Soil (S2)	Soil No.1
Poisson's Ratio	0.15	0.15	0.45	0.495	0.45
Density, T/m3	2.8	2.7	2	1.992	1.9
Vs, m/s	2800	800	600	133.8	360
H, km	16.04	1.8	0.14	0.010	0.010

The shear wave velocities of hard rock, weathered rock, liquefiable soil and top soil are 3500 m/s (Class A), 762 m/s (Class B or C), 600 m/s (Class B), 183 m/s (Class D or E) and 250 m/s (Class D) which are classified by National Earthquake Hazards Reduction Program (NEHRP) site classes, respectively. The ground water table is at the bottom of Soil No.1 or the top of Soil No.2.

The dynamic excess pore water pressures due to the vertical and horizontal components of earthquakes decrease slightly from 35.05 kPa to 34.25 kPa and from 22.06 kPa to 21.24 kPa with the decrease in the degree of saturation from 0.9999 to 0.85 (Table 2 and Figure 1). Mu is the Poisson's ratio, second line in Table 1.

Table 2 Variations of the dynamic excess pore water pressures, Poisson's ratio and shear wave velocity with the degree of saturation.

s	0.9999	0.999	0.995	0.95	0.9	0.85
Mu	0.49995	0.4995	0.4975	0.475	0.45	0.425
Vsaw (m/s)	1016.6	409.4	183.1	60.3	42.8	35.2
Hz (kPa)	35.05	35.05	35	34.96	34.5	34.25
hx (kPa)	22.06	22.02	21.93	21.59	21.4	21.24

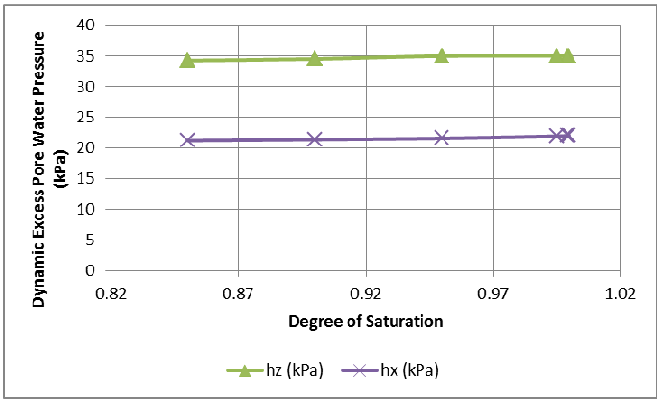

Fig. 1 Variations of the dynamic excess pore water pressures with the degree of saturation

The liquefiable depth, which can be defined as the ratio of the dynamic excess pore water pressure and the unit weight of the soil No.1, is the maximum depth with the effective stress changing from negative values to zero value.

If the unit weight of the soil No.1 is 19.62 kN/m2, the liquefiable depth due to vertical and horizontal components of earthquakes slightly decreases from 1.786 to 1.746 and from 1.124 to 1.083 with the decrease in the degree of saturation from 0.9999 to 0.85, respectively. So, for the 1989 Loma Prieta earthquake with the earthquake magnitude of 7.0, the liquefactions are taking place only for places where the depths of the ground water tables are equal to or less than 1.7m and 1.1m, for the vertical and horizontal components of earthquakes, respectively.

Table 3 Variations of the liquefiable depth with the degree of saturation.

s	0.9999	0.999	0.995	0.95	0.9	0.85
hzv (m)	1.786	1.786	1.784	1.782	1.758	1.746
hzh (m)	1.124	1.122	1.118	1.100	1.090	1.083

Liquefaction was also observed even in unsaturated zone (Sheng, (15)). The soils frequently encountered in geotechnical engineering are unsaturated. The liquefiable soil layer under the phreatic surface is not, as usual assumed fully saturated, but in a partially saturated states (Tsukamoto and Ishihara, (16) and (17)). In-situ test results, including compression wave velocity measurements indicate that partial saturation conditions may exit below ground water level for a few meters due to presence of air bubbles (Ishihara et al. (18); and Nakazawa et al. (19)) or gas bubbles in marine sediments and oil sands (Mathiroban et al (20)).

The factors of safety due to the vertical and horizontal components of earthquakes against liquefaction are the ratios of the thickness of soil No.1 and the liquefiable depths due to the vertical and horizontal components of earthquakes, respectively, as

$$F_{sLz} = \frac{h_{zs1}}{h_{lz}} = \frac{h_{zs1}\gamma_{s1}}{h_{ez}} \tag{6}$$

$$F_{sLx} = \frac{h_{zs1}}{h_{lx}} = \frac{h_{zs1}\gamma_{s1}}{h_{ex}} \tag{7}$$

The factors of safety increase with the increase in the unit weights of the soil No.1, so there are currently many methods to compact the soil No.1 or top soil, e.g. vibro-flotation methods, vibro-stone column (SC) and dynamic compaction (DC) techniques supplemented with wick drains to densify and mitigate liquefaction in saturated sands and non-plastic silty soils [Shenthan et al. (21)].

If the percentage of air bubbles in the solid-air-water mixtures is 0.53% and the vertical and horizontal frequencies of earthquakes are equal to 1.0 Hz, the dynamic excess pore water pressures due to the vertical and horizontal components of earthquakes very slightly decrease from 35.00 kPa to 34.975 kPa and from 21.92 kPa to 21.829 kPa, and the shear wave velocity of the solid-air-water (SAW) mixtures decreases from 175 m/s to 116.1 m/s with the increase in the porosity from 0.2 to 0.8 of the solid-air-water (SAW) mixture, respectively (Table 4 and Figure 2).

If the percentage of air bubbles in the solid-air-water mixtures is 1% and the vertical and horizontal frequencies of earthquakes are equal to 1.0 Hz, the dynamic excess pore water pressures due to the vertical and horizontal components of earthquakes increase from 17.51 kPa to 519.20 kPa and from 11.03 kPa to 298.52 kPa with the increase in the thickness of the liquefiable soil (soil No.2) from 5m to 150m, respectively (Table 5 and Figure 3).

Table 4 Variations of the shear wave velocity and the dynamic excess pore water pressures with the porosity

n	0.2	0.3	0.4	0.5	0.6	0.7	0.8
Vsaw	175	148.4	133.8	125.04	119.8	116.9	116.1
hz(kPa)	35	34.994	34.99	34.984	34.982	34.98	34.975
hx(kPa)	21.92	21.88	21.86	21.848	21.837	21.831	21.829

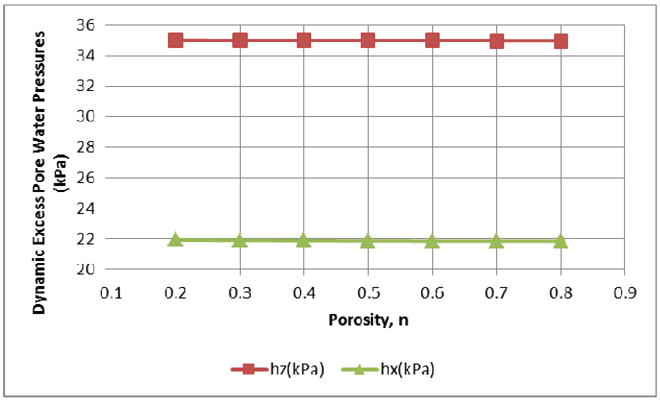

Fig. 2 Variations of the shear wave velocity and the dynamic excess pore water pressures with the porosity.

Table 5 Variations of the dynamic excess pore water pressures with the thickness of the liquefiable soil (soil No.2).

H s2 (m)	5	10	15	20	50	100	150
hz(kPa)	17.51	35	52.48	69.95	174.45	347.52	519.2
hx(kPa)	11.03	21.93	32.77	43.54	106.53	205.8	298.52

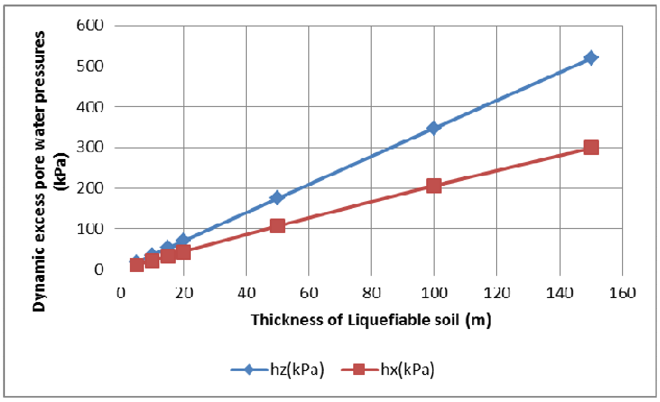

Fig. 3 Variations of the dynamic excess pore water pressures with the thickness of the liquefiable soil (soil No.2).

If the percentage of air bubbles in the solid-air-water mixtures is 1% and the porosity of 0.4 of the solid-air-water (SAW) mixtures, the dynamic excess pore water pressures due to the vertical and horizontal components of earthquakes decrease from 140 kPa to 6.998 kPa and from 87.46 kPa to 4.373 kPa with the increase in the frequencies of earthquakes in the vertical and horizontal directions from 0.025 Hz to 0.5 Hz, respectively (Table 6 and Figure 4). Note that the relationship between the corner frequencies and the moment magnitude are based on Hank et al. (22) and Alkinson et al. (23). The relationships between the dynamic excess pore water pressures and the moment magnitude are shown in Figures (5) and (6).

Table 6 Variations of the dynamic excess pore water pressures with the frequencies of earthquakes in vertical and horizontal directions.

fz or fx	0.025	0.05	0.1	0.15	0.2	0.3	0.5
hz(kPa)	140	69.98	34.99	23.33	17.494	11.663	6.998
hx(kPa)	87.46	43.73	21.86	14.58	10.932	7.288	4.373
Mmz	8.68	8.08	7.48	7.13	6.88	6.52	6.08
Mmx	8.3	7.69	7.09	6.7	6.49	6.14	5.69

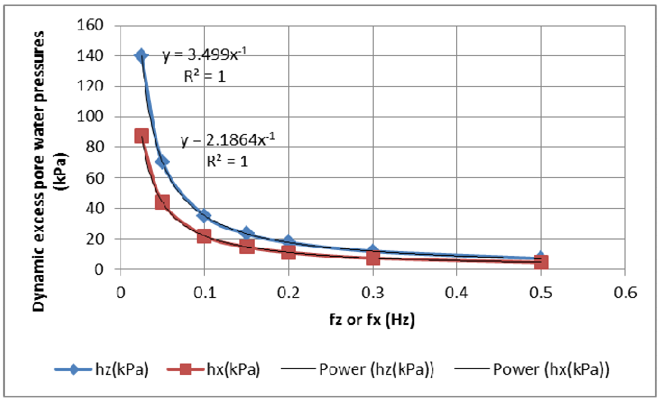

Fig. 4 Variations of the dynamic excess pore water pressures with the frequencies of earthquakes in vertical and horizontal directions.

The relationships between the dynamic pore water pressures due to the vertical and horizontal components of earthquakes and the vertical and horizontal frequencies of earthquakes have the power forms with the squares of the correlation coefficients of 1.0, respectively:

$$h_{ez} = \frac{3.499}{f_z} \tag{8}$$

$$h_{ex} = \frac{2.1864}{f_x} \tag{9}$$

If the percentage of air bubbles in the solid-air-water mixtures is 1%, the frequencies due to the vertical and horizontal components of earthquakes of 0.1 Hz, and the porosity of 0.4 of the solid-air-water (SAW) mixtures, the dynamic excess pore water pressures due to the vertical and horizontal components of earthquakes decrease from 46.4 kPa to 27.17 kPa and from 28.77 kPa to 17.08 kPa with the increase in the fault depth of earthquakes from 12 km to 25 km, respectively (Table 7 and Figure 7).

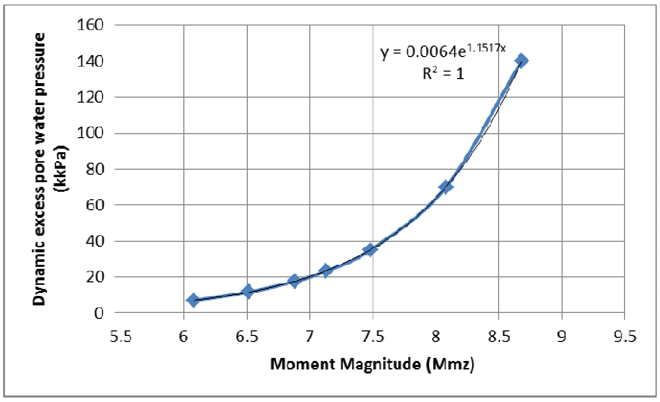

Fig.5 Variation of the dynamic excess pore water pressure with moment mangitude due to vertical component of earthquake

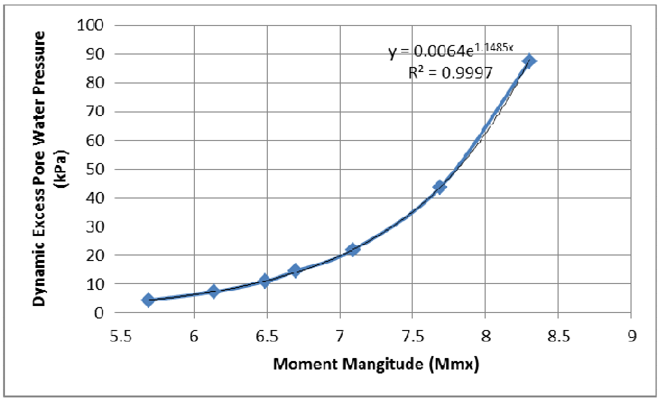

Fig.6 Variation of the dynamic excess pore water pressure with moment mangitude due to horizontal component of earthquake

The relationships between the dynamic pore water pressures due to the vertical and horizontal components of earthquakes and the vertical and horizontal moment magnitudes of earthquakes have the exponential forms with the squares of the correlation coefficients of 1.0 and 0.9997, respectively:

$$h_{ez} = 0.0064e^{1.1517\,Mmz} \tag{10}$$

$$h_{ex} = 0.0064e^{1.1485\,Mmx} \tag{11}$$

Table 7 Variations of the dynamic excess pore water pressures with the fault depth of earthquakes.

HF (km)	12	15	18	20	22	25
hz(kPa)	46.44	39.91	34.99	32.33	30.05	27.173
hx(kPa)	28.77	24.85	21.86	20.24	18.848	17.08

The relationships between the dynamic pore water pressures due to the vertical and horizontal components of earthquakes and the vertical and horizontal frequencies of earthquakes have the polynomial forms with the squares of the correlation coefficients of 0.9995 and 0.9996, respectively:

$$h_{ez} = 0.0594 h_F^{\ 2} - 3.6598 h_F + 81.679 \quad (9)$$

$$h_{ex} = 0.0035 h_F^{\ 2} - 2.1873 h_F + 48.893 \quad (10)$$

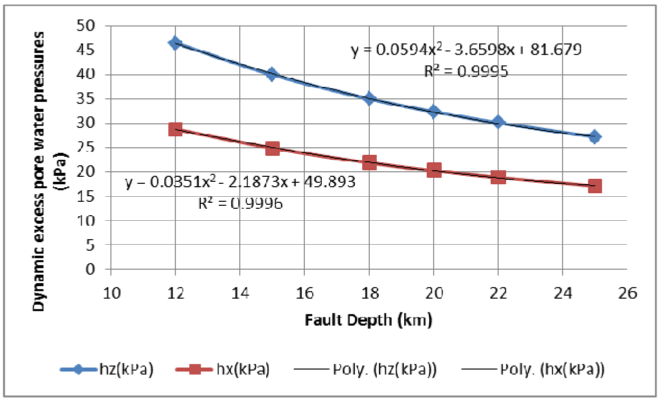

Fig. 7 Variations of the dynamic excess pore water pressures with the fault depth of earthquakes.

If the percentage of air bubbles in the solid-air-water mixtures is 1%, the frequencies due to the vertical and horizontal components of earthquakes of 0.1 Hz, and the porosity of 0.4 of the solid-air-water (SAW) mixtures, the dynamic excess pore water pressures due to the vertical and horizontal components of earthquakes decrease from 39.55 kPa to 31.89 kPa and from 24.51 kPa to 19.98 kPa with the increase in the thickness of weathered rock from 1.0 km to 2.5 km, respectively (Table 8 and Figure 8).

Table 8 Variations of the dynamic excess pore water pressures with the thickness of weathered rock.

Hwr	1	1.2	1.5	1.8	2	2.5
Hr	16.84	16.64	16.34	16.04	15.85	15.34
hz (kPa)	39.55	38.16	36.51	34.99	34.04	31.89
hx(kPa)	24.51	23.79	22.79	21.86	21.29	19.98

The increase in thickness of weathered rock of 1.5 km is equal to the decrease in the thickness of the hard rock of 1.5 km in order to keep the constant fault depth of 18 km for the Loma Prieta earthquake (Table 8).

If the percentage of air bubbles in the solid-air-water mixtures is 1%, the frequencies due to the vertical and horizontal components of earthquakes of 0.1 Hz, and the porosity of 0.4 of the solid-air-water (SAW) mixtures, the dynamic excess pore water pressures due to the vertical and horizontal components of earthquakes increase from 27.69 kPa to 43.61 kPa and from 17.40 kPa to 27.08 kPa with the increase in the shear wave velocity of hard rock from 2500 m/s to 5000 m/s, respectively (Table 9 and Figure 9).

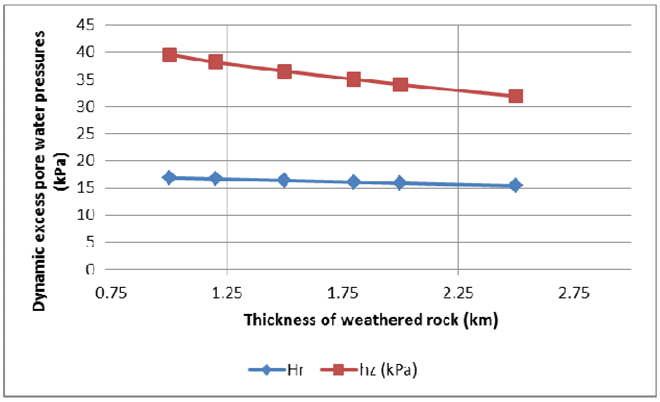

Fig. 8 Variations of the dynamic excess pore water pressures with the thickness of weathered rock.

Table 9 Variations of the dynamic excess pore water pressures with the shear wave velocity of hard rock.

Vs r (m/s)	2500	3000	3500	4000	5000
hz (kPa)	27.69	31.53	34.99	38.13	43.61
hx(kPa)	17.4	19.75	21.86	23.77	27.08

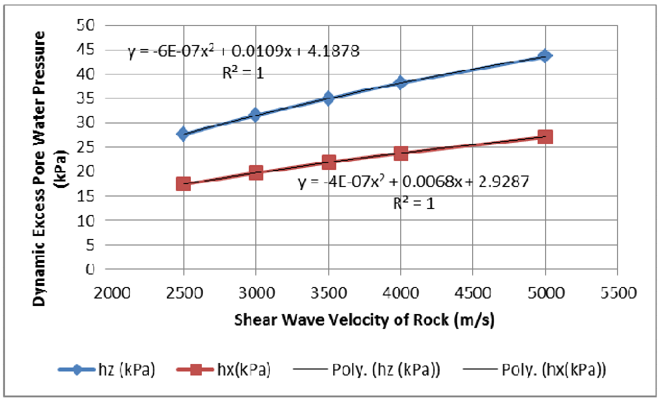

Fig. 9 Variations of the dynamic excess pore water pressures with the shear wave velocity of hard rock.

The relationships between the dynamic pore water pressures due to the vertical and horizontal components of earthquakes and the shear wave velocity of hard rock have the polynomial forms with the squares of the correlation coefficients of 1.0, respectively:

$$h_{ez} = -0.0000006 V_s^{\ 2} + 0.0109 V_s + 4.1878 \quad (9)$$

$$h_{ex} = -0.0000004 V_s^{\ 2} + 0.0068 V_s + 2.9287 \quad (10)$$

IV. Discussions and Conclusions

The value of the Poisson's ratio of the liquefiable soil is dominated by the degree of saturation of the solid-air-water (SAW) mixtures. The Poisson's ratio of the fully saturated soils is 0.5 and decrease with the increase in the percentage of air bubbles if the SAW mixtures. For example, the Poisson's ratio of the SAW mixture with 1% air bubbles is 0.495, which is higher than that of dry loose sand of 0.33.

The shear wave velocity of the solid-air-water mixtures substantially decreases from 1016.7 m/s to 35.2 m/s with the decrease in the degree of saturation from 0.9999 to 0.85, but the dynamic excess pore water pressures due to the vertical and horizontal components of earthquakes slightly decrease from 35.05 kPa to 34.25 kPa, and from 22.06 kPa to 21.24 kPa, respectively.

Dynamic excess pore water pressures due to the vertical and horizontal components of earthquakes increase with the increase in the degree of saturation, shear wave velocity of hard rock and thickness of the liquefiable soil, and with the decrease in the fault depth of earthquakes, thickness of weathered rock, frequencies of the earthquakes and the porosity of the solid-air-water (SAW) mixtures.

The relationships between the dynamic excess pore water pressures due to the vertical and horizontal components of earthquakes and the frequencies, and fault depths of earthquakes have the power and polynomial forms, respectively.

Dynamic excess pore water pressures due to vertical and horizontal components of earthquakes based on the dynamic soil masses and dynamic water heights depends on many parameters: e.g. number, thickness, properties of soil or rock layers, and fault depth and corner frequencies of earthquakes.

Liquefaction potential depends on the thickness and properties of the soil layers above the ground water table and the dynamic excess pore water pressures.

Factors of safety due to vertical and horizontal components of earthquakes against the liquefaction increase with the increase in the thickness and unit weights of the soils above the ground water table and with the decrease in the excess pore water pressures.

REFERENCES

[1] Z. Zhang, C.Cho, Q. Pan and X. Lu. "Experimental Investigation on Excess Pore Water Pressure in Soft Soil-Foundations under Minor Shocks", *International Journal of Engineering and Applied Sciences,* 5:4 2009*,* pp. 259-263.

[2] A.C. Trandafir, K. Sassa and H. Fukuoka. "A Computational Method for Residual Excess Pore Pressure Response in Sand under Cyclic Loading". *Annuals of Disas. Prev. Res.Inst.,* Kyoto Univ., No. 45 B-1, 2002, 9 p.

[3] T. Matsui, H. Ohara and T. Ito. "Cyclic Stress-Strain History and Shear Characteristics of Clay". *Journal of the Geotechnical Engineering Division,* ASCE, 106, GT10 (180), pp. 1101-1120**.**

[4] H. Matsuda, S. Ohara and S. Sano. "Settlement and Excess Pore Water Pressure of Saturated Clay Induced by Cyclic Shear with Different Periods". *Pro. Of Ninth World Conference on Earthquake Engineering, Aug. 2-9, 1988.* Tokyo-Kyoto, Japan (Vol.III), pp. 83-88.

[5] A. Namdar, and M.K. Pelkoo. "Evaluation of Pore Water Pressure Characteristics in Embankment Model". *Pacific Journal of Science and Technology.* 10(1) 2009, pp. 501-506.

[6] R. Kayen., R.B. Seed, R.E. Moss, O. Cetin, Y. Tanaka, and K. Tokimatsu. "Global Shear Wave Velocity Database for Probabilistic Assessment of the Initiation of Seismic-Soil Liquefaction", *DRAFT for 11th International Conference on Soil Dynamics & Earthquake Engineering*, Berkeley, CA January 7-9, 2004, 7 p.

[7] H.V.P. Truong. "Behaviour of Small Footings Subjected to Horizontal Vibratory Loading". Ph.D. Thesis, the University of Melbourne, 1993, Australia.

[8] H.V.P. Truong. "Added Soil Mass and Ratio of Damping For Vertical and Horizontal Vibration", *Proc. Of 11th Conference on Science and Technology*, University of Technology in Saigon, Vietnam National University, Vietnam, 2009, pp. 24-30.

[9] H.V.P. Truong. "Effects of Damping and Dynamic Soil Mass on Footing Vibration", *Proc. Geo-Shanghai International Conference in June 2010* (or ASCE Geotechnical Special Publications), 2010, pp. 177-183.

[10] H.V.P. Truong. "Effects of Air Bubbles, Solids and Frequency on Tsunami Waves". *Proc. 14th Asian Regional Conference on Soil Mechanics and Geotechnical Engineering*, in Hong Kong *in* May 2011 (2011), Paper No.334.

[11] H.V.P. Truong. "Dynamic Soil Mass or Added Soil Mass and Dynamic Rock Mass in Foundation Designs, and Dynamic Soil Amplification", *Proc. Of 14th World Congress on Advances in Structural Engineering and Mechanics* (ASEMPlus), 18-22 September 2011, Seoul Korea, pp. 4893-490.

[12] H.V.P. Truong. "Natural Frequencies of Soil-Foundation Systems and Soil Layers". *Proc. 12th Conference on Science and Technology*, University of Technology in Saigon, Vietnam National University, Vietnam, 2011, Paper No. D08, 8 p.

[13] H.V.P. Truong. "Vertical and horizontal dynamic water heights in tsunamis -Air Bubbles to Save Lives", *Proc. 12th Conference on Science and Technology, University of Technology in Saigon*, Vietnam National University, Vietnam, 2011, Paper No. D09, 10 p.

[14] H.V.P. Truong. "Liquefaction and lateral spreading by dynamic soil mass for earthquakes" *International Journal of Geology* (Accepted for publication) 2012.

[15] Z.J. Sheng, Theoretical soil mechanics, China Waterpower Press, 1999.

[16] Y. Tsukamoto, K. Ishihara, H. Nakazawa.; K. Kamada and Y. Huang,. Resistance of partly saturated sand to liquefaction with reference to longitudinal and shear wave velocities. *Soils and Foundations*. Vol. 42, No. 6, 2002, 93-104.

[17] Y. Tsukamoto, T. Kamata, K. Tatsuoka and K. Ishihara, K.. Undrained flow characteristics of partially saturated sandy soils in triaxial tests. *Proc. 4th International Conference on Earthquake Geotechnical Engineering*:, 2007, 25-28.

[18] K. Ishihara, H. Tsuchiya, Y. Huang, Y. and K. Kamada, . Recent studies on Liquefaction Resistance of Sand-Effect of Saturation. *Proc. Fourth International Conference on Recent Advances in Geotechnical Earthquake Engineering and Soil Dynamics and Symposium in Honour of Professor W.D. Liam Finn*. San Diego, California, Keynote Lecturer, 2001.

[19] H. Nakazawa, K. Ishihara, Y. Tsukamoto and T. Kamada . Case studies on Evaluation of Liquefaction Resistance of Imperfectly Saturated Soil Deposits. *Proc. Conf. Cyclic Behaviour of Soils and Liquefaction Phenomena*, Germany, 2004.

[20] S. Mathiroban, and J. Grozic. A model to predict the undrained behaviour of Loose Gassy Sand. *Proc. 57 Geotech. Conf.,* Session 6G: 2004, 16-22.

[21] T.,Shenthan, R.G. Nashed, S. Thevanayagam,and G.R. Martin. "Liquefaction Mitigation in Silty Soils Using Composite Stone Columns and Dynamic Compaction" . *Seismic Vulnerability of the Highway System*, 2004, pp. 207-220.

[22] T. C. Hank and D.M. Boore. "Moment-magnitude relations in theory and practice" *Journal of Geophysical Research*, Vol. 89, No. B7 (1984), pp. 6229-6235.

[23] G. M. Atkinson and D. M. Boore. "Earthquake Ground-Motion Prediction Equations for Eastern North America" *Bulletin of the Seismological Society of America*, Vol.96, No.6, 2006, pp. 2181-2205.

Phuong H.V. Truong, born in Saigon Vietnam, received his Bachelor of Civil Engineering from the National Technical Center in Saigon Vietnam, Master of Engineering (Geotechnical Engineering) from the Asian Institute of Technology (AIT) in Bangkok Thailand, Graduate Diploma in International

Trade from the Deakin University in Melbourne, Victoria Australia; and Doctor of Philosophy (Ph.D.) in Civil Engineering from the University of Melbourne in Melbourne, Victoria Australia. He had worked for many companies in different countries; mainly (i) as civil/geotechnical engineer for the Roads Construction Authority (VicRoads) for 13 years, and received the 1988 Bicentennial Award from the Roads Construction Authority (VicRoads) in Victoria Australia in 1988; and (ii) as transportation engineer for the California Department of Transportation (Caltrans) in California USA for 9 years; and published more than 24 papers in civil engineering and geotechnical engineering. His current main research interests are soil dynamics, geotechnical earthquake engineering and tsunamis.